

## Iterative modelling, migration and inversion (IMMI): the role of well calibration in the context of high geological complexity

Sergio Romahn and Kristopher Innanen  
CREWES

### Summary

Iterative modelling, migration and inversion (IMMI) aims to incorporate standard processing techniques into the process of full waveform inversion (FWI). IMMI proposes the use of any depth migration method to obtain the gradient, while FWI uses a two-way wave migration, commonly reverse time migration (RTM). IMMI uses well calibration to scale the gradient, instead of applying a line search to find the scalar or an approximation of the inverse Hessian matrix. We used a phase shift plus interpolation (PSPI) migration with a deconvolution imaging condition that works as a gain correction. We show the suitability of estimating the subsurface velocity model by applying IMMI's approach using synthetic examples with increasingly geological complexity. We found consistently low errors in the well calibration location, even in the most complex settings. This suggests that the gradient obtained by applying PSPI migration points to the correct direction to minimize the objective function, and that well calibration provides an optimal scale. This is promising in the context of reservoir characterization, where we may have many control wells. We found that IMMI satisfactorily performs in the presence of moderate lateral velocity changes. The results, for the scenario of strong lateral velocity changes, indicate that well calibration is a worthy option providing that the well is representative of the geology in the zone of interest or we have enough control wells in the inversion area.

### Introduction

Lailly (1983) and Tarantola (1984) provided the mathematical basis for full waveform seismic inversion. They showed that FWI and migration are strongly linked, in what Margrave et al. (2010) call the fundamental theorem of FWI, which is summarized in Equation 1.

$$\delta v(x, z) = \lambda \nabla_v \phi_k(x, z, \omega) = \lambda \int \sum_{s,r} \omega^2 \hat{\Psi}_s(x, z, \omega) \delta \hat{\Psi}_{r(s),k}^*(x, z, \omega) d\omega \quad (1)$$

Where  $\delta v$  is the velocity update,  $\lambda$  is a scalar constant,  $\nabla$  is the gradient with respect to the velocity model  $v$ ,  $\phi$  is the objective function for iteration  $k$ ,  $\omega$  is angular frequency,  $\Psi_s$  is a model of the source wavefield for source  $s$  propagated to all  $(x, z)$ ,  $\delta \Psi_r$  is the  $k$ th data residual for source  $s$  back propagated to all  $(x, z)$ ,  $*$  means complex conjugation. The residual  $\delta \Psi_r$  is the difference between the observed data and the modeled data. The objective function measures the difference between the recorded data and the modelled data at the  $k$ th iteration (Equation 2).

$$\phi_k = \sum_{s,r} (\Psi - \Psi_k)^2 \quad (2)$$

Equation 1 says that the gradient of the objective function ( $rv\_k$ ) is formed by correlating the time inverse residuals propagated into the medium with the source field propagated into the medium. This is the core of FWI. The gradient is the element that contains the direction of the velocity update in the minimization scheme. The other element is the inverse Hessian or an approximation of it. If the inverse Hessian is replaced by a scalar  $\lambda$ , the mathematical effort is reduced to the gradient or steepest-descent method.  $\lambda$  scales the gradient to be converted into a velocity perturbation.  $\lambda$  is commonly estimated by a line-search method which requires an extra forward problem per shot (Virieux and Operto, 2009). Margrave et al. (2010) described the process of FWI as an iterative cycle that involves four main steps shown in figure 1.

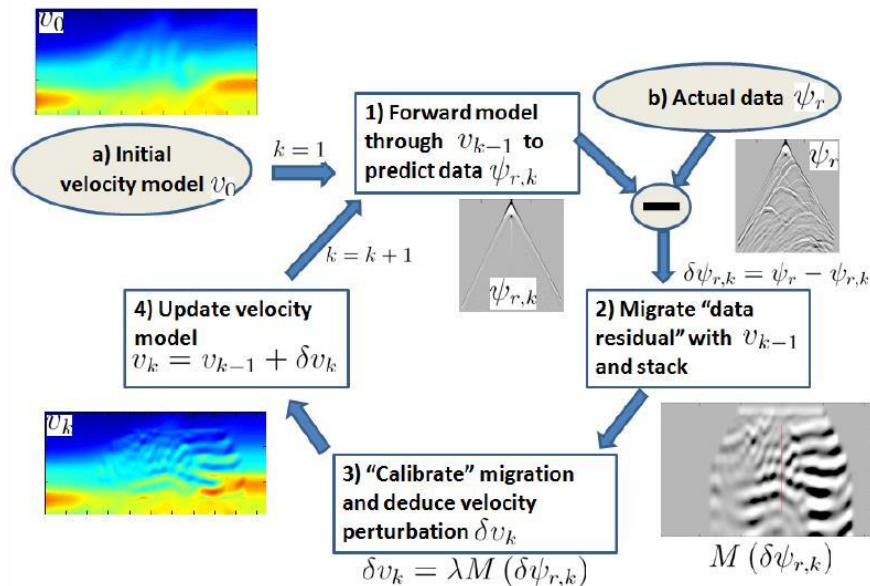


FIG. 1. The cycle of FWI (Margrave et al., 2010)

- 1) Generating synthetic seismic data (predicted data) from an initial model  $v_0$ , and calculation of the data residual.
- 2) Pre-stack depth migration using the current velocity model of the data residual and stack. This step provides the gradient or update direction.
- 3) Scaling or calibrating the gradient that produces the velocity perturbation.
- 4) Updating current velocity model which will be used in the next iteration.

IMMI, introduced by Margrave et al. (2012), was thought as an alternative for accomplishing FWI by using tools already available and widely used by the industry. Examples of IMMI's philosophy are the application of any depth migration method and the incorporation of well information for scaling the gradient. Furthermore; the authors suggest that using a deconvolution imaging condition, instead of the correlation used in RTM, may achieve something very similar to the role of the main diagonal elements of the inverse Hessian, which is a gain correction as illustrated by Shin et al. (2001). Pan et al. (2014) applied the IMMI method, compared the crosscorrelation and deconvolution imaging conditions, and showed that using a deconvolution based gradient can compensate the geometrical spreading.

Following IMMI's approach, we use the phase shift plus interpolation migration method (one-way wave migration) with a deconvolution imaging condition to obtain the gradient. PSPI, presented by Gazdag and Sguazzero (1984), allows selecting a range of frequencies of interest which is very convenient to explore frequency employment strategies in FWI. Pratt (1999) suggested that starting the inversion using low frequencies and then moving to higher frequencies may help to avoid local minima. We will follow this

strategy. The scale  $\lambda$  in Equation 1, is estimated in the form of a match filter that equates the size of the gradient to the size of the velocity residual in a well location. The velocity residual is the difference between the well velocity and the current velocity model.

## Method

The observed shots for this experiment are the idealized version of the ones that would be recorded on the field. We generated these shots by using an acoustic finite-difference algorithm to propagate the wavefield. A minimum phase wavelet with a dominant frequency of 20 Hz was used as seismic source. The sources are placed every 50 m from 2100 to 9250 m, giving 144 shots in total. Receiver stations are located along the whole model every 10 m, and all of them are kept alive for each shot.

### *First iteration*

The initial velocity model was generated by applying a Gaussian smoother of width 290 meters to the true velocity model. The initial velocity model provides no more than 2 Hz of geological information while the true velocity model mainly contains information between 1 and 30 Hz, with the main events around 12 Hz. The seismic data has a dominant frequency of around 15 Hz and provides information between 7 and 25 Hz. There is gap between 2 and 5 Hz where neither the initial model nor the seismic data contribute. Modelled shots were generated by using the initial model. The difference between the observed and the modelled shots is the data residual. We obtain a data residual per shot, then they are migrated in depth by using the PSPI method, which allows introducing a specific frequency range. We used frequencies between 1 and 5 Hz for the first iteration. A mute, before stacking the residuals, is commonly applied to avoid migration artifacts. The product of stacking the migrated data residuals is the gradient. The next step is to scale or calibrate the gradient. We use well C to perform this process. The well calibration technique was described by Margrave et al. (2010). Firstly, the difference  $\delta vel$ , between the well and model velocities is calculated. The second step is to estimate the amplitude scalar  $a$  and a phase rotation  $\phi$  that make the gradient trace  $g$  more like  $\delta vel$ . The scalar  $a$  is found such that  $\delta vel - ag$  is minimized by least squares. Finally, a convolutional match filter is obtained with  $a$  and  $\phi$ . This match filter is applied to every gradient trace to obtain the velocity update.

### *More iteration*

The inputs for the next iterations are the frequency range and the updated velocity model. The frequency range was increased by 1 Hz each iteration. We stopped the inversion at the 10th iteration, because the error in the model does not decrease anymore after that point.

## Examples

We evaluated the performance of the well calibration C technique in three different geological settings (figure 2). For the simplest model constituted by horizontal layers (Model 1), the inversion is able to recover the most important features of the true model and the error is consistently low in the whole model. When moderate lateral velocities are found such as in Model 2, the smallest errors occur around the calibration well and the inverted model is a good representation of the true model. When strong lateral velocity changes are present such as in Model 3, the inversion produces good results in the calibration well, however the error increases as we go away from the well specially in the zones of the high velocity bodies.

## Conclusions

The gradient, calculated with a one-way wave migration method (PSPI) under a deconvolution imaging condition, points to the correct direction to minimize the objective function in the FWI scheme. We

showed that the use of well information to calibrate the gradient produces a suitable velocity perturbation to update the model. This was confirmed by the consistently low error in the well location even for the most geological complex model. Well calibration satisfactorily performs in the presence of moderate lateral velocity changes, such as in Model 1 and 2. The error decreases each iteration as we go to higher frequencies. The inversion is able to define the target and the main geological features. When we have strong lateral velocity variations, such as in the Marmousi Model, the inversion works properly in the shallow part, and is able to recover the main features in the deeper part. However, the velocity tends to be underestimated as we go to deeper zones. We found that well calibration can be used in these settings, providing that the well is representative of the geology of the area of interest. These results suggest that a calibration that varies horizontally (providing more control wells) and with depth would be a worthy option to obtain better velocity updates.

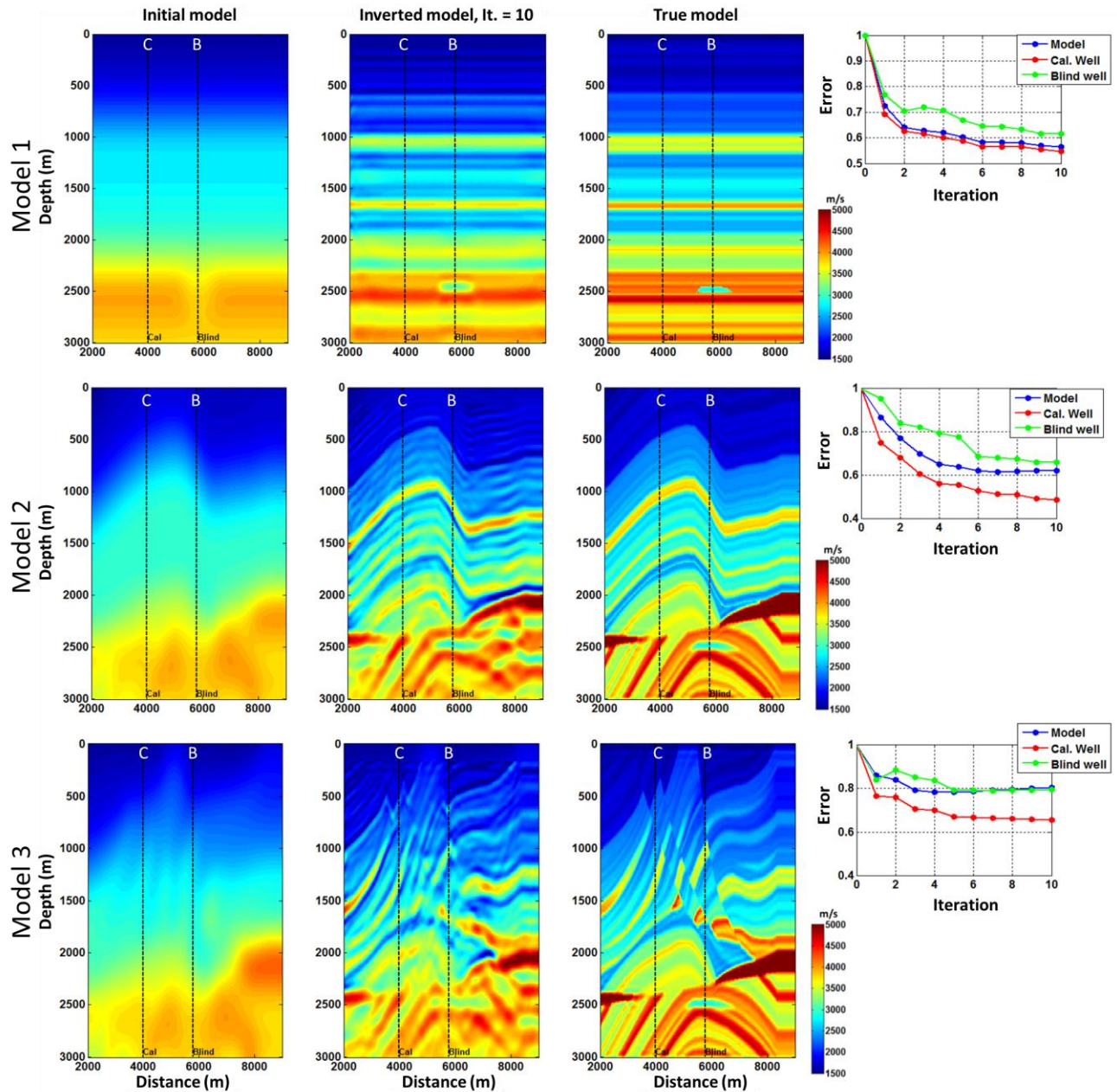


FIG. 2. Comparison among initial, inverted and true velocity models.

## Acknowledgements

We thank the sponsors of CREWES for their support. We also acknowledge support from NSERC through the grant CRDPJ 461179-13. Author 1 thanks PEMEX and the government of Mexico for founding his research.

## References

Gazdag, J., and Sguazzero, P., 1984, Migration of seismic data by phase shift plus interpolation: *Geophysics*, 49, No. 2, 124–131.

Lailly, P., 1983, The seismic inverse problem as a sequence of before stack migration: *SIAM*, 206–220.

Margrave, G. F., Ferguson, R. J., and Hogan, C. M., 2010, Full-waveform inversion with wave equation migration and well control: CREWES Research Report, 22.

Margrave, G. F., Innanen, K. A., and Yedlin, M., 2012, A perspective on full-waveform inversion: CREWES Research Report, 24.

Pan, W., Margrave, G. F., and Innanen, K. A., 2014, Iterative modeling migration and inversion (immi): Combining full waveform inversion with standard inversion methodology: 84th Ann. Internat. Mtg., SEG, Expanded Abstracts, 938–943.

Pratt, R. G., 1999, Seismic waveform inversion in the frequency domain, part 1: Theory and verification in a physical scale model: *Geophysics*, 64, No. 3, 888–901.

Shin, C., Yoon, K., Marfurt, K. J., Park, K., Yang, D., Lim, H. Y., Chung, S., and Shin, S., 2001, Efficient calculation of a partial-derivative wavefield using reciprocity for seismic imaging and inversion: *Geophysics*, 66, No. 6, 1856–1863.

Tarantola, A., 1984, Inversion of seismic reflection data in the acoustic approximation: *Geophysics*, 49, 1259–1266.

Virieux, A., and Operto, S., 2009, An overview of full-waveform inversion in exploration geophysics: *Geophysics*, 74, 1259–1266.